Analytical solution for Joule–Thomson cooling during CO_2 geo-sequestration in depleted oil and gas reservoirs

Simon A. Mathias[a]*, Jon G. Gluyas[a], Curtis M. Oldenburg[b], Chin-Fu Tsang[b]

[a]Department of Earth Sciences, Durham University, Durham, UK
[b]Earth Sciences Division, Lawrence Berkeley National Laboratory, Berkeley, CA, USA

ABSTRACT

Mathematical tools are needed to screen out sites where Joule Thomson cooling is a prohibitive factor for CO^2 geo-sequestration and to design approaches to mitigate the effect. In this paper, a simple analytical solution is developed by invoking steady-state flow and constant thermophysical properties. The analytical solution allows fast evaluation of spatiotemporal temperature fields, resulting from constant-rate CO_2 injection. The applicability of the analytical solution is demonstrated by comparison with non-isothermal simulation results from the reservoir simulator TOUGH2. Analysis confirms that for an injection rate of 3 kgs−1 (0.1MTyr−1) into moderately warm(>40°C) and permeable formations(>10^{-14}m^2 (10 mD)), JTC is unlikely to be a problem for initial reservoir pressures as low as2 MPa (290 psi).

Keywords: Joule–Thomson cooling
Geologic carbon sequestration
Depleted gas reservoirs

1. Introduction

Depleted oil and gas reservoirs (DOGRs) represent a significant portion of the global portfolio of target formations currently under consideration for CO_2 geo-sequestration (Benson and Cook, 2005). There are two major advantages associated with DOGRs:(1) they have been extensively characterized during exploration, appraisal and production; (2) they are already proven as potentially long- term traps for buoyant fluids owing to their ability to store oil and gas over tens to hundreds of millions of years(Maloney and Briceno, 2009). However, low pore-pressures, characteristic of depletion- drive reservoirs at cessation of production, will lead to significant Joule–Thomson cooling (JTC) when large pressure gradients are developed due to CO_2 injection. JTC is the name given to the drop in temperature that occurs when a real gas such as CO_2 expands from high pressure to low pressure at constant enthalpy (i.e., adiabatic expansion) (see Oldenburg, 2007b, for further detail). Of particular concern is the severe loss of injectivity that may develop due to freezing of pore fluids (e.g., native brine)and/or the generation of CO_2 or CH_4 hydrates, effectively rendering the injection well dysfunctional (Oldenburg, 2007b). Mathematical tools are needed to identify and evaluate sites where JTC is a prohibitive factor for CO_2 geo-sequestration and to aid in the design of approaches to mitigate the effect.

Previously JTC during CO_2 geo-sequestration has been explored using laboratory experiments (Maloney and Briceno, 2009) and numerical simulation (Oldenburg, 2007a; Bielinski et al., 2008; André et al., 2010). For wider accessibility and application, analytical solutions are preferable, especially those that can be implemented in simple spreadsheet software (e.g. Oldenburg, 2007b; Mathias et al., 2009a,b). Unfortunately, analytical solution of the full JTC problem is not possible due to the non-linear coupling between the associated fluid flow and thermal transport equations. However, for the low pressures of interest, the Joule–Thomson coefficient for CO_2 remains relatively constant (see André et al., 2010, Fig. 1). It is therefore hypothesized that meaningful results can be obtained when thermophysical properties are assumed constant and uniform.

In this paper, a simple analytical solution is developed by invoking steady-state flow and constant thermophysical properties. The analytical solution allows fast evaluation of spatiotemporal temperature fields resulting from constant-rate CO_2 injection. The applicability of the analytical solution is demonstrated by comparison with fully coupled and transient non-isothermal simulation results from the reservoir simulator TOUGH2/EOS7C (Oldenburg et al., 2004a). Sensitivity analysis of the analytical solution is explored to provide insight into the importance of JTC for DOGRs.

2. The mathematical model

Consider the constant-rate injection of fluid from a fully penetrating injection well into an infinite, homogenous and isotropic, insulated and confined formation. As mentioned previously, for the low pressures of interest, the Joule–Thomson coefficient for CO_2 remains relatively constant. It is therefore hypothesized that meaningful results can be obtained when thermophysical properties are

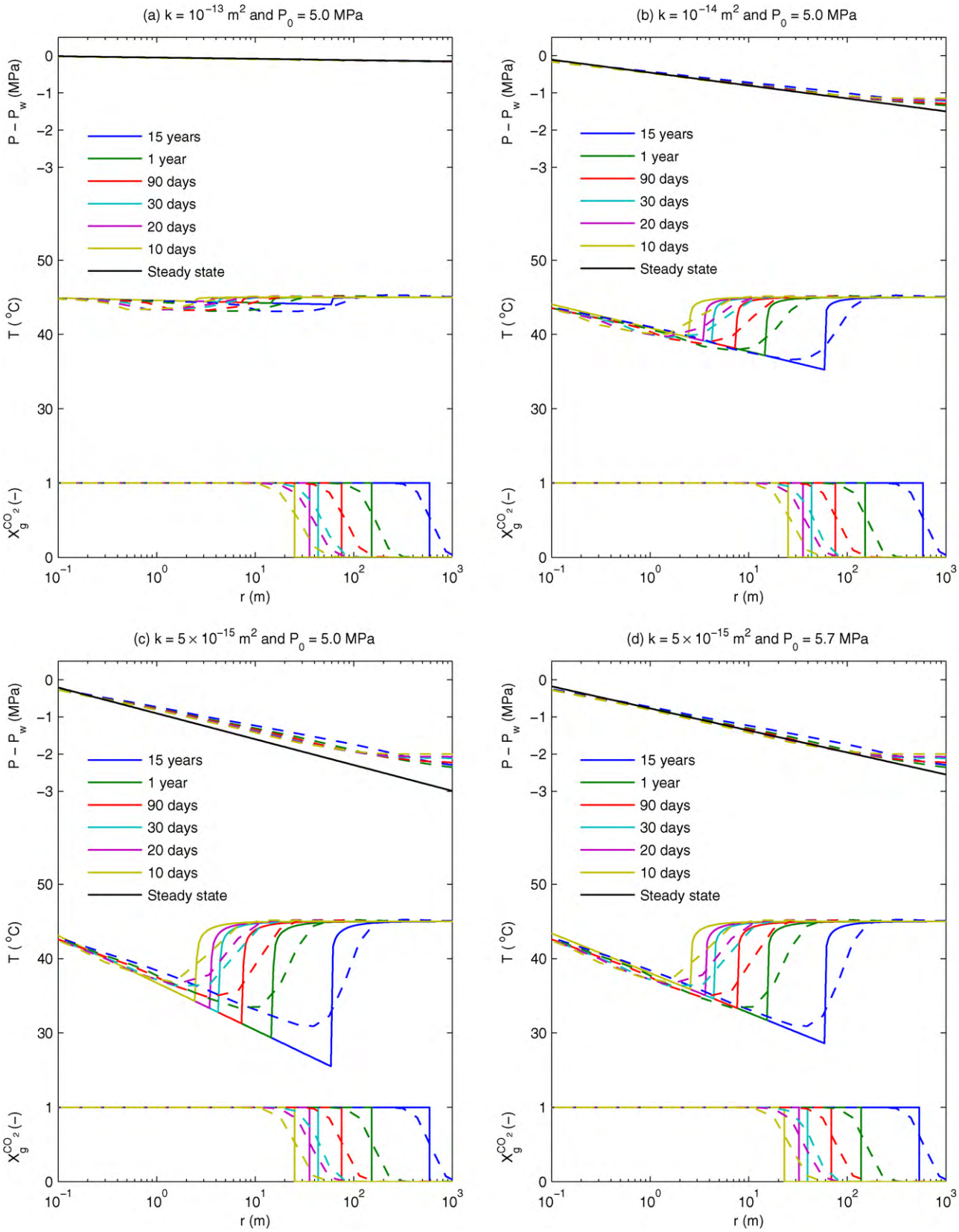

Fig. 1. Profiles of pressure difference, $P - P_w$, temperature, T, and CO_2 mass fraction in the gas phase, $X_g^{CO_2}$, at six different times. The dashed lines are from the TOUGH2 simulation previously presented by Oldenburg (2007a). The solid lines are from the analytical solution with pressure, temperature and $X_g^{CO_2}$ calculated from Eqs. (5), (21) and (6), respectively. See Table 1 for parameter values.

assumed constant and uniform. For mathematical tractability, it is further assumed that the flow-field is single-phase and steady-state. The single-phase assumption is meaningful here because the temperature front, caused by injection, lags behind the advection front due to retardation caused by the specific heat capacity of the rock and connate water. Therefore activity of concern should generally be contained within the single-phase zone that develops around the injection well. The steady-state assumption is conservative when looking at cooling because the transient increase in pressure has a heating effect and transient compressibility effects initially reduce spatial pressure gradients. Assuming fluid, rock and connate water to be in local thermal equilibrium and ignoring longitudinal thermal conduction, the simplified heat transport problem can be written as

$$[n(1-S_r)\rho_f c_f + nS_r\rho_w c_w + (1-n)\rho_s c_s]\frac{\partial T}{\partial t} = -q\rho_f c_f\left[\frac{\partial T}{\partial r} - \alpha\frac{\partial P}{\partial r}\right] \tag{1}$$

subjected to the initial and boundary conditions:

$$\begin{aligned} &T = T_0, \quad r \geq r_w, \quad t = 0 \\ &T = T_w, \quad r = r_w, \quad t > 0 \end{aligned} \tag{2}$$

where n is the porosity, S_r is the residual water saturation, $\rho_f\,(\mathrm{ML^{-3}})$ is the fluid density, $c_f\,(\mathrm{L^2T^{-2}\theta^{-1}})$ is the fluid specific heat capacity, $\rho_w\,(\mathrm{ML^{-3}})$ is the density of water, $c_w\,(\mathrm{L^2T^{-2}\theta^{-1}})$ is the specific heat capacity of water, $\rho_s\,(\mathrm{ML^{-3}})$ is the rock density, $c_s\,(\mathrm{L^2T^{-2}\theta^{-1}})$ is the rock specific heat capacity, $T\,(\theta)$ is the fluid temperature, $q\,(\mathrm{LT^{-1}})$ is the bulk fluid flow per unit area, $\alpha\,(\mathrm{M^{-1}LT^2}\theta)$ is the Joule–Thomson coefficient, $P\,(\mathrm{ML^{-1}T^{-2}})$ is the fluid pressure, $r\,(\mathrm{L})$ is radial distance from the injection well, $H\,(\mathrm{L})$ is the formation thickness, $T_0\,(\theta)$ is the background temperature, $T_w\,(\theta)$ is the fluid temperature at the injection well and $r_w\,(\mathrm{L})$ is the well radius.

The pressure gradient is obtained from Darcy's law:

$$\frac{\partial P}{\partial r} = -\frac{\mu q}{k_r k} \tag{3}$$

where $\mu\ (\mathrm{ML^{-1}T^{-1}})$ is fluid viscosity, k_r is relative permeability (a reduction factor to take into account the residual saturation of water) and $k\ (\mathrm{L^2})$ is permeability. Ignoring compressibility effects and assuming single-phase flow, the fluid flux is obtained from

$$q = \frac{M_0}{2\pi r H\rho_f} \tag{4}$$

where $M_0\ (\mathrm{MT^{-1}})$ is the mass injection rate and $H\,(\mathrm{L})$ is the formation thickness.

Substituting Eq. (4) into Eq. (3) and integrating with respect to r leads to the Thiem equation for the pressure distribution

$$P = P_w + \frac{M_0\mu}{2\pi H\rho_f k_r k}\ln\left(\frac{r_w}{r}\right) \tag{5}$$

where $P_w\ (\mathrm{ML^{-1}T^{-2}})$ is the pressure in the injection well.

By continuity, the radial distance to the CO_2 front, $r_F\,(\mathrm{L})$, can be found from

$$r_F = \left[\frac{M_0 t}{\pi H n(1-S_r)\rho_f}\right]^{1/2} \tag{6}$$

Our final set of equations represent the coupling of a transient heat equation with a steady-state flow equation. Substituting the following dimensionless transformations

$$r_D = \frac{r}{r_w} \tag{7}$$

$$t_D = \left[\frac{c_f}{n(1-S_r)\rho_f c_f + nS_r\rho_w c_w + (1-n)\rho_s c_s}\right]\frac{M_0 t}{2\pi H r_w^2} \tag{8}$$

$$T_D = \frac{2\pi H k_r k(T-T_0)\rho_f}{\alpha\mu M_0} \tag{9}$$

$$T_{wD} = \frac{2\pi H k_r k(T_w-T_0)\rho_f}{\alpha\mu M_0} \tag{10}$$

leads to:

$$\frac{\partial T_D}{\partial t_D} = -\frac{1}{r_D}\left[\frac{\partial T_D}{\partial r_D} + \frac{1}{r_D}\right] \tag{11}$$

$$\begin{aligned} &T_D = 0, \quad r_D \geq 1, \quad t_D = 0 \\ &T_D = T_{wD}, \quad r_D = 1, \quad t_D > 0 \end{aligned} \tag{12}$$

Applying the Laplace transform

$$\hat{T}_D(s) = \int_0^\infty T_D(t)\ \exp(-st_D)\,dt_D \tag{13}$$

allows the above problem to further reduce to

$$s\hat{T}_D = -\frac{1}{r_D}\left[\frac{\partial \hat{T}_D}{\partial r_D} + \frac{1}{sr_D}\right] \tag{14}$$

$$\hat{T}_D = \frac{T_{wD}}{s}, \qquad r_D = 1 \tag{15}$$

which has the analytical solution

$$\hat{T}_D(s, r_D) = \frac{1}{2s}\ \exp\left(-\frac{sr_D^2}{2}\right)\left[E_1\left(-\frac{sr_D^2}{2}\right) - E_1\left(-\frac{s}{2}\right)\right] + \frac{T_{wD}}{s}\ \exp\left[-\frac{s}{2}(r_D^2-1)\right] \tag{16}$$

where E_1 denotes the En-function with $n=1$, which relates to the exponential integral function, $\mathrm{Ei}(x)$, via $E_1(x) = -\mathrm{Ei}(-x)$.

To invert Eq. (16) back to the time-domain, consider the Laplace transform identity

$$L^{-1}\left\{e^{-as}E_1(-as)\right\} = \frac{1}{t_D - a} \tag{17}$$

It follows that

$$L^{-1}\left\{\frac{1}{2s}\ \exp\left(-\frac{sr_D^2}{2}\right)E_1\left(-\frac{sr_D^2}{2}\right)\right\} = \int_0^{t_D}\frac{d\tau}{2\tau - r_D^2} = \frac{1}{2}\ \ln\left(1 - \frac{2t_D}{r_D^2}\right) \tag{18}$$

and

$$L^{-1}\left\{\frac{1}{2s}\ \exp\left(-\frac{s}{2}\right)E_1\left(-\frac{s}{2}\right)\right\} = \int_0^{t_D}\frac{d\tau}{2\tau - 1} = \frac{1}{2}\ \ln(1-2t_D) \tag{19}$$

and consequently that

$$L^{-1}\left\{-\frac{1}{2s}\ \exp\left(-\frac{sr_D^2}{2}\right)E_1\left(-\frac{s}{2}\right)\right\} = \begin{cases} 0, & t_D < \dfrac{r_D^2-1}{2} \\ -\dfrac{1}{2}\ln(r_D^2 - 2t_D), & t_D \geq \dfrac{r_D^2-1}{2} \end{cases} \tag{20}$$

Considering Eqs. (18) and (20) with Eq. (16) finally yields

$$T_D(r_D, t_D) = \begin{cases} \dfrac{1}{2}\ \ln\left(1 - \dfrac{2t_D}{r_D^2}\right), & t_D < \dfrac{r_D^2-1}{2} \\ \dfrac{1}{2}\ln\left(\dfrac{1}{r_D^2}\right) + T_{wD}, & t_D \geq \dfrac{r_D^2-1}{2} \end{cases} \tag{21}$$

The discontinuity occurs at the location of the minimum temperature, T_{min} (θ). Setting $t_D = (r_D^2 - 1)/2$, it can be seen that the minimum temperature is directly calculated from

$$T_{min} = -\frac{\alpha \mu M_0}{4\pi H k_r k \rho_f} \times \ln\left\{\left[\frac{c_f}{n(1-S_r)\rho_f c_f + nS_r\rho_w c_w + (1-n)\rho_s c_s}\right]\frac{M_0 t}{\pi H r_w^2} + 1\right\} + \begin{cases} T_0, & T_0 \le T_w \\ T_w, & T_0 > T_w \end{cases} \quad (22)$$

3. Comparison with TOUGH2/EOS7C

To evaluate the applicability of the above analytical solution, calculated results are compared to fully coupled and transient non-isothermal numerical simulation results from TOUGH2/EOS7C (as presented by Oldenburg, 2007a, Figs. 5–7). The scenarios considered are based on those used in the economic feasibility study for carbon sequestration with enhanced gas recovery in the Rio Vista Gas Field, Sacramento Valley, California (Oldenburg et al., 2004b). The model parameters used are given in Table 1. Note that all the parameters used in the present calculations are as previously specified by Oldenburg (2007a) with the exception of the CO_2 thermophysical properties: ρ_f, μ, c_f and α, which were calculated using the web-resource of Lemmon et al. (2003).

Comparison plots of pressure, temperature and CO_2 mass fraction in the gas phase, $X_g^{CO_2}$ are presented in Fig. 1a–d. The well pressure, P_w, for the analytical solution is undefined due to the assumption of steady-state flow. Therefore all pressures, P, are plotted as a difference from the well pressure, P_w.

Fig. 1a shows results for the high permeability formation where $k = 10^{-13}$ m^2. The TOUGH2 pressure difference, $P - P_w$, and the advective front of the CO_2 plume (see plot of $X_g^{CO_2}$) are seen to be well approximated by the analytical solution. The analytical solution assumes a sharp interface whereas TOUGH2's $X_g^{CO_2}$ distribution is smoother due to the dispersive effects of molecular diffusion, mobility difference between the injection and formation fluids and numerical dispersion. The analytical solution underestimates the resulting temperature drop by around half but both models are forecasting close to negligible temperature drops for this scenario.

A formation of lower permeability (10^{-14} m^2) is considered in Fig. 1b. The pressure difference is well approximated by the analytical solution in the inner region around the well although some minor deviation starts to occur at radii greater than 10 m. The advection fronts of the CO_2 plume are also well approximated, disregarding dispersion effects. Because permeability has been reduced, the pressure gradients have increased. Consequently, the Joule–Thomson related temperature drop is enhanced. The analytical solution provides a good approximation to the TOUGH2 simulation results without the dispersive effects seen at the cooling front. The additional smoothing in temperature predicted by TOUGH2 is due to proper inclusion of thermal conduction in conjunction with numerical dispersion.

Results for a formation of very low permeability (5×10^{-15} m^2) is presented in Fig. 1c. The story is the same as in Fig. 1b except that the lower permeability leads to even higher pressure gradients and consequently greater pressure declines due to the Joule–Thomson effect. It is apparent that the analytical solution is overestimating pressure gradient, as compared to TOUGH2, and consequently, marginally overestimating the temperature decline. The reason is due to the assumption of constant thermophysical properties. Because the permeability is so low there is substantial pressure buildup. In the full reservoir simulation (i.e. TOUGH2), this leads to increased fluid density, a reduction (as compared to the analytical solution) in the volume of fluid being forced in, a reduction in pressure gradient and consequently a reduction in temperature decline. Such an effect can be compensated for in the analytical solution by increasing the assumed value of reservoir pressure, P_0, by 14% (see Fig. 1d).

The comparison between the analytical solution and the full reservoir simulations using TOUGH2 presented in Fig. 1a–d confirm that the analytical solution offers a useful approximation to the full problem using parameters describing scenarios of practical interest. The assumption of constant thermophysical properties is conservative in this context, leading to an overestimate of the temperature decline caused by Joule–Thomson cooling. It follows that the analytical solution is suitable for bounded analysis relating to the suitability of DOGRs.

Table 1
Assumed model parameters.

Property	Value	
Formation thickness, H (m)	50	
Porosity, n	0.30	
Permeability, k (m^2)	Varies	
Rock density, ρ_s (kg m^{-3})	2600	
Rock heat capacity, c_s (J kg^{-1} K^{-1})	1000	
CO_2 injection rate, M_0 (kg s^{-1})	3	
Well radius, r_w (m)	0.05	
Injection and reservoir temperature, T_w, T_0 (°C)	45	
Residual water saturation, S_r	0.2	
Relative permeability, k_r	1	
Water density, ρ_w (kg m^{-3})	992	
Water heat capacity, c_w (J kg^{-1} K^{-1})	4037	
Reservoir pressure, P_0 (MPa)	5.0	5.7
CO_2 density, ρ_f (kg m^{-3})	109	131
CO_2 viscosity, μ (μPa s)	17.2	17.7
CO_2 heat capacity, c_f (J kg^{-1} K^{-1})	798	825
Joule–Thomson coefficient, α (K MPa^{-1})	9.13	9.01

4. Pressure and temperature sensitivity

A major advantage of the analytical solution over TOUGH2 is that the minimum temperature for a given scenario, T_{min}, can be evaluated using a single calculation based on Eq. (22). Consequently, much broader sensitivity analysis can be more easily evaluated. Plots of T_{min} are presented in Fig. 2, for a range of reservoir pressures, P_0, and temperatures, T_0, for the three formations previously considered after 50 years of injecting CO_2 for the scenario described in Table 1 (but with CO_2 thermophysical properties calculated for each value of T_0 and P_0 using Lemmon et al., 2003). The limitation of the analytical solution is that couplings between properties, pressure, temperature and composition are not modeled.

As expected, the temperature declines are larger where initial pressures are lowest. As observed in Fig. 1a–d, temperature decline is seen to reduce with increasing permeability. However, temperature declines are greatest for the high temperature scenario. This is surprising because the Joule–Thomson coefficient, α, diminishes with increasing temperature (see André et al., 2010). The larger temperature declines are caused by the increased pressure gradients resulting from the injection of greater volumes of low density CO_2 (recall discussion in the previous section).

As stated previously, the main concern associated with JTC is the loss of injectivity caused by hydrate formation. Sun and Duan (2005) compiled a large set of experimental data from the literature concerning pressure–temperature equilibria for CO_2 and CH_4 hydrates. The shaded region in Fig. 2 was interpolated from Sun and Duan (2005, Figs. 6 and 7) and denotes the region in which CO_2 and/or CH_4 hydrates may develop. For moderately warm and permeable formations (i.e., $T_0 > 40$ °C and $k > 10^{-14}$ m^2), JTC is unlikely to be a problem for initial reservoir pressures as low as 2 MPa in

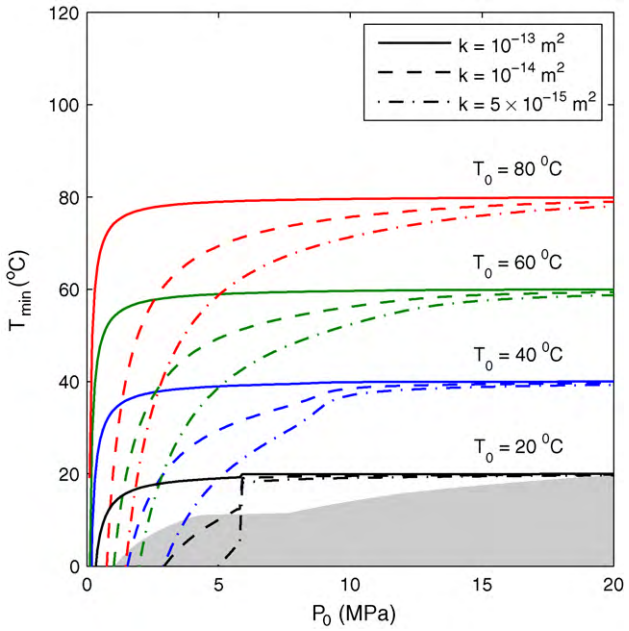

Fig. 2. Plot of minimum temperature, T_{min} (calculated from Eq. (22)), for a range of background pressures, P_0, background temperatures, T_0 and permeabilities, k after 50 years of injection. See Table 1 for other parameters. The shaded region bounds the region in which CO_2 and/or CH_4 hydrates are likely to develop (after Sun and Duan, 2005).

on-shore reservoirs. However, for cold formations ($T < 20\,^{\circ}C$), e.g. sub-sea, JTC may cause hydrate formations where initial reservoir pressures are as high as 6 MPa. But at such low temperatures, high pressures also become a concern for hydrate formation (Sun and Duan, 2005).

5. Summary and conclusions

Depleted reservoirs are often considered for CO_2 storage. However, there is concern that characteristic low pressures may lead to significant Joule–Thomson cooling resulting in CO_2 and/or CH_4 hydrate formation and consequently, prohibitively poor injectivity. Previously, forecasting temperature change associated with Joule–Thomson cooling in CO_2 storage reservoirs required expensive numerical reservoir simulation. This paper presents a new analytical solution (Eq. (22)) to the problem providing convenient and accessible insight into the underlying physics and allowing broad parameter sensitivity analysis to be easily facilitated. Analysis confirms that for an injection rate of 3 kg s^{-1} (0.1 MT yr^{-1}) into moderately warm (>40 °C) and permeable formations (>10^{-14} m^2 (10 mD)), JTC is unlikely to be a problem for initial reservoir pressures as low as 2 MPa (290 psi). However, for cold formations (<20 °C), JTC may cause hydrate formation where initial reservoir pressures are as high as 6 MPa (870 psi).

Acknowledgments

We thank internal LBNL reviewer, Andrea Cortis for his constructive comments. Partial support for this work was provided by LBNL under US DOE Contract No. DE-AC02-05CH11231.

References

André, L., Azaroual, M., Menjoz, A., 2010. Numerical Simulations of the thermal impact of supercritical CO_2 injection on chemical reactivity in a carbonate saline Reservoir. Transp. Porous Media 82, 247–274.

Benson, S., Cook, P., 2005. Underground geological storage. In: Metz, B., Davidson, O., de Coninck, H., Loos, M., Meyer, L. (Eds.), IPCC Special Report on Carbon Dioxide Capture and Storage. Cambridge University Press, pp. 195–276.

Bielinski, A., Kopp, A., Schutt, H., Class, H., 2008. Monitoring of CO_2 plumes during storage in geological formations using temperature signals: numerical investigation. Int. J. Greenhouse Gas Control 2, 319–328.

Lemmon, E., McLinden, M., Friend, D., 2003. Thermophysical properties of fluid systems. In: Linstrom, P.J., Mallard, W.G. (Eds.), NIST Chemistry WebBook, NIST Standard Reference Database Number. National Institute of Standards and Technology, 69, Gaithersburg, Maryland, http://webbook.nist.gov/.

Maloney, D.R., Briceno, M., 2009. Experimental investigation of cooling effects resulting from injecting high pressure liquid or supercritical CO_2 into a low pressure gas reservoir. Petrophysics 50, 335–344.

Mathias, S.A., Hardisty, P.E., Trudell, M.R., Zimmerman, R.W., 2009a. Approximate solutions for pressure buildup during CO_2 injection in brine aquifers. Transp. Porous Media 79, 265–284.

Mathias, S.A., Hardisty, P.E., Trudell, M.R., Zimmerman, R.W., 2009b. Screening and selection of sites for CO_2 sequestration based on pressure buildup. Int. J. Greenhouse Gas Control 3, 577–585.

Oldenburg, C.M., 2007a. Joule–Thomson cooling due to CO_2 injection into natural gas reservoirs. Energy Convers. Manage. 48, 1808–1815.

Oldenburg, C.M., 2007b. Screening and ranking framework for geologic CO_2 storage site selection on the basis of health, safety, and environmental risk. Environ. Geol. 54, 1687–1694.

Oldenburg, C.M., Moridis, G.J., Spycher, N., Pruess, K., 2004a. EOS7C Version 1.0: TOUGH2 Module for Carbon Dioxide or Nitrogen in Natural Gas (Methane) Reservoirs. Lawrence Berkeley National Laboratory Report LBNL-56589, March 2004.

Oldenburg, C.M., Stevens, S.J., Benson, S.M., 2004b. Economic feasibility of carbon sequestration with enhanced gas recovery (CSEGR). Energy 29, 1413–1422.

Sun, R., Duan, Z., 2005. Prediction of CH_4 and CO_2 hydrate phase equilibrium and cage occupancy from ab initio intermolecular potentials. Geochim. Cosmochim. Acta 69, 4411–4424.